Composites

JOURNAL OF
biomaterials
applications

Journal of Biomaterials Applications
2021, Vol. 35(8) 1043–1060

DOI: 10.1177/0885328220972219
journals.sagepub.com/home/jba
SAGE

Biomimetic bone-like composites as osteo-odonto-keratoprosthesis skirt substitutes

Venkata Avadhanam[1,2], Ganesh Ingavle[3,4], Yishan Zheng[3], Sandeep Kumar[3], Christopher Liu[1,5,6] and Susan Sandeman[3]

Abstract

Osteo-odonto-keratoprostheses, incorporating dental laminate material as an anchoring skirt around a central poly (methyl methacrylate) (PMMA) optic, have been used to replace the cornea for many years. However, there are many intricacies associated with the use of autologous dental laminate material, surgical complexity and skirt erosion. Tissue engineering approaches to bone replacement may offer suitable alternatives in osteo-odonto-keratoprosthesis (OOKP) surgery. In this study, a hydrogel polymer composite was investigated as a synthetic substitute for the OOKP skirt. A novel high strength interpenetrating network (IPN) hydrogel composite with nano-crystalline hydroxyapatite (nHAp) coated poly (lactic-co-glycolic acid) PLGA microspheres was created to mimic the alveo-dental lamina by employing agarose and poly(ethylene glycol) diacrylate (PEGDA) polymers. The incorporation of nHAp coated PLGA microspheres into the hybrid IPN network provide a micro-environment similar to that of skeletal tissues and improve cellular response. Agarose was used as a first network to encapsulate keratocytes/3T3 fibroblasts and PEGDA (6000 Da) was used as a second network with varying concentrations (20 and 40 wt %) to produce a strong and biocompatible scaffold. An increased concentration of either agarose or PEG-DA and incorporation of nHAp coated PLGA microspheres led to an increase in the elastic modulus. The IPN hydrogel combinations supported the adhesion and proliferation of both fibroblast and ocular human keratocyte cell types during in *in-vitro* testing. The cells endured the encapsulation process into the IPN and remained viable at 1 week post-encapsulation in the presence of nHAp coated microspheres. The material did not induce significant production of inflammatory cytokine IL-6 in comparison to a positive control ($p < 0.05$) indicating non-inflammatory potential. The nHAp encapsulated composite IPN hydrogels are mechanically strong, cell supportive, non-inflammatory materials supporting their development as OOKP skirt substitutes using a new approach to dental laminate biomimicry in the OOKP skirt material.

Keywords

Interpenetrating network hydrogel, bio-mineralisation, biomimetic, hydroxyapatite coating, osteo-odonto-keratoprosthesis

Introduction

The cornea is a specialized tissue with distinct anatomical and physiological features, which enable its transparency and barrier function. The regular and compact arrangement of stromal collagen fibres, avascularity, lack of nerve fibre myelination and the presence of the endothelial pump, which keeps the cornea in a dehydrated state, contribute to corneal transparency.[1] For the maintenance of its health and transparency, smooth and complete blinking, good tear production and normal corneal endothelial pump function are essential. Corneal transparency can be affected in

[1]Brighton and Sussex Medical School, Brighton, UK
[2]Bristol Eye Hospital, Bristol, UK
[3]School of Pharmacy and Biomolecular Sciences, University of Brighton, Brighton, UK
[4]Symbiosis Centre for Stem Cell Research, Symbiosis International University, Pune, India
[5]Sussex Eye Hospital, Brighton, UK
[6]Tongdean Eye Clinic, Hove, UK

Corresponding author:
Susan Sandeman, School of Pharmacy and Biomolecular Sciences, University of Brighton, Huxley Building, Lewes Road, Brighton BN2 4AT, UK.
Email: s.sandeman@brighton.ac.uk

diseases of the cornea and in some conditions involving the conjunctiva, eyelids and anterior segment.[2]

Being the anterior most structure of the globe, the cornea is exposed to a variety of threats from environmental, microbial and physical agents and injury. Any insult to the corneal tissue can lead to swelling and scarring, which eventually results in its opacification.[3] In a recent study, corneal blindness was calculated to be prevalent in 4.9 million (12%) out of the 39 million total blind population across the globe.[4] Corneal transplantation from a cadaveric donor can replace the diseased cornea and restore vision in the majority of cases. The corneal grafts survive better in non-inflammatory and non-vascularised disease states such as corneal opacities, keratoconus and dystrophies. The 5 year graft survival in these cases can be up to 90%.[5] However, corneal graft survival is severely reduced in cases where there is persisting ocular inflammation, eyelid abnormalities, and extensive ocular damage due to physical, chemical and thermal injuries with tissue loss, chronic ocular surface diseases and recurrent viral infections. Corneal graft survival beyond 5 years in high risk cases can be as low as 54%.[5]

A keratoprosthesis (KPro) is indicated when corneal transplantation carries a high risk or if multiple grafts have failed. A KPro is a synthetic device implanted into the eye to replace the diseased cornea. Usually, a KPro contains a 'skirt' for its integration into the ocular tissues where it is deployed and an 'optic' to allow light transmission. Scores of device models have been tested with variations in the skirt and optic design and materials used (Supplementary Table 1).[4] Earlier attempts to treat corneal blindness started with synthetic materials such as glass nearly two hundred years ago.[6–10] The "core and optic" concept was further explored in mid-19th century using a number of materials, including glass,[11,12] quartz,[13] glass with polymer,[13] and quartz crystal with platinum ring.[13] Later, advances in polymers encouraged other investigators to try substances like polyurethane and polytetrafluoroethylene (PTFE),[14] silicone and Dacron,[15] ceramic,[16] PMMA disk,[17,18] PMMA in nut and bolt form,[19,20] PMMA and Teflon,[21] polycarbonate,[14,22] PMMA and titanium,[23] PMMA and Dacron,[24–26] hydrogels[13,27,28] as described in Supplementary Table 1.

Since the performance of the synthetic skirt material was disappointing, some investigators have tried to harness the superior bio-integrable properties of biological tissues within the eye. Strampelli observed the tolerance to gutta percha in the root canal for indefinite periods but not in the soft tissues.[29] This led him to use the root-alveolar complex as the KPro skirt and insertion of a PMMA optical cylinder in the root canal.[30] He also used oral mucosa to cover the prosthesis. Strampelli used the cross section of the root canal and alveolar bone tissue to retain the cylinder by employing dental cement.[29] Falcinelli modified the procedure and the present day OOKP is based on his modifications.[31]

Edentulous patients cannot benefit from OOKP; hence, investigators have extended their search for tooth alternatives in OOKP technique. Casey used costal cartilage,[30] and Temprano used tibial cortex fragment instead of the tooth.[32] Tibial KPro is still used as an alternative to OOKP in some centres.[33,34] Pintucci used a dacron skirt with PMMA optical cylinder and implanted the device as a two-stage procedure in a surgically similar fashion to the present OOKP technique.[35] However, the device suffered extrusions.[36] Only two devices, the Boston type-1 KPro and OOKP have shown clinical success. However, Falcinelli's modified OOKP continues to be used and has proven to be a stable device over the long term. The Boston KPro contains a synthetic titanium skirt and poly-methyl-methacrylate (PMMA) optic, while the OOKP is partly biological in constitution and contains an alveo-dental plate skirt (tooth and bone composite tissue) and PMMA optic.[37] The indications and surgical techniques for these devices are varied as are their outcomes and complications. Table 1 illustrates the main differences between the Boston type 1 KPro and the OOKP. A detailed account of the various KPros and OOKPs have been given in our previous publication.[38]

OOKP is performed in two or three stages.[39,40] The first stage involves preparation of the device from a single rooted front tooth with an adjoining piece of either maxillary or mandibular of bone followed by grafting of a patch of buccal mucosa onto the ocular surface (Figure 1(a) to (c)). The OOKP lamina is prepared from the root of the tooth with its adjoining alveolar bone tissue, which is prepared as a plate. A central hole is on the broader surface of the alveo-dental plate and the optical cylinder is inserted via the dentinal side of the lamina (having its dentine side sitting on the cornea). An implantable plate is prepared from the tooth-bone complex and a transparent optical cylinder made of PMMA is inserted into the centre after drilling an aperture for tight-fit (Figure 1(a)). This alveo-dento-acrylic complex or OOKP lamina is embedded in the sub-orbicular tissue pocket of the contralateral inferior eyelid for connective tissue ingrowth into the lamina.[41] In the same procedure or prior to laminar preparation a piece of buccal mucous membrane graft (BMG) is obtained and sutured to cover the anterior eye. The OOKP lamina and BMG are left for at least three months for maturation and vascular investment before proceeding to the next stage of the operation (Figure 1(a)). In the later stages of the operation, the BMG is partially dissected from the

Table 1. Comparison of Boston type-1 and OOKP.

Feature	Boston type-1	OOKP
Materials	Optic – PMMA Skirt – Titanium Carrier – Cadaveric cornea	Optic – PMMA Skirt – Alveo-dental plate Carrier – Fibrovascular tissue
Device models	Phakic and aphakic	Aphakic
Design	The Boston type 1 KPro uses a donor cornea between a central stem and a back plate	The OOKP uses osteo-dental lamina derived from an extracted tooth root and attached alveolar bone removed from the patient's jaw
Onlay cover for the device	Absent	Buccal mucosal patch graft
Surgical steps	Boston type-1 KPro surgical procedure is technically less challenging but has a less follow-up record	OOKP surgery is a complex multi-staged procedure, labour-intensive, and relatively invasive procedure requiring dental expertise. It requires life-long follow up
Indications	Only in wet blinking eyes without eyelid anomalies	Severely dry and non-blinking eyes with eyelid anomalies
Infection	B-KPro carries a long-term risk of infection	It has the least risk of infection, making it more suitable for a lifelong support to the optical part of KPro
Pros and cons	1. Synthetic device and no loss of tooth 2. Simple surgical technique and short learning curve 3. Bio-integration is unpredictable 4. Easy repeatability of the procedure as the device is fully synthetic 5. Exterior of the device is unprotected and prone to corneal melts 6. Reduced longevity of the device compared to OOKP	1. Loss of tooth and buccal mucosa 2. Complex and multistage surgical procedure and surgeons must go through a steep learning curve to get enough expertise 3. Excellent bio-integration 4. Repetition of the OOKP is challenging as it needs a new lamina. 5. Device is protected by a robust buccal mucosal graft 6. Most durable KPro compared to all the devices used so far

superior half of the globe, the central cornea is trephined, and anterior segment structures are removed, and the device is implanted into the eye (Figure 1(b)). The mucosa is replaced and an opening is made in its centre for outward projection of the front stem of the optical cylinder (Figure 1(c)).[41]

OOKP is a highly successful KPro. However, it requires multidisciplinary teamwork by various ophthalmic sub-specialists and allied staff. Further surgical revisions are needed for each patient after device implantation. The OOKP device is high maintenance, demanding both the patient's and surgeon's long-term commitment and causes significant surgical morbidity to the patient. Hence, this service requires specialised care at dedicated units. Over the years, cumulative procedural costs, theatre time and follow up schedules make the OOKP an expensive surgery.[38]

OOKP offers distinct advantages over other synthetic devices. In OOKP, the ocular surface is covered with a robust buccal mucosa. Thus, it not only protects the device, but also nourishes its skeletal framework. Being biological tissue, the integrity of the laminar skirt is excellent and unparalleled to any other synthetic materials. Nonetheless, the lamina is a skeletal tissue and undergoes resorption, which can reduce its longevity in the eye. Employing a synthetic skirt material in place of the tooth provides several benefits by avoiding oral trauma, minimising surgical steps and reducing the cost and burden of the complex surgery. Most importantly laminar resorption is eliminated and in cases where repetition and device replacement are required, an off the shelf, readily implantable synthetic device would be a significant improvement to the current status. Having the mucosal cover over the synthetic skirt can also protect it from external agents and can prevent device extrusion. These principles were also adopted in earlier KPros like the Pintcucci KPro.[35] A synthetic skirt for the OOKP must therefore be developed in accordance with its surgical paradigm, which should ideally mimic the properties of the alveo-dentate lamina. Various bioactive and bioinert materials such as silicone, teflon, dacron, Poly(2-hydroxyethyl methacrylate) (polyHEMA) hydrogels and titanium, have been developed for KPro skirt substitution.[26,42–47] However, the majority of these devices were not effective because they lacked either the required mechanical

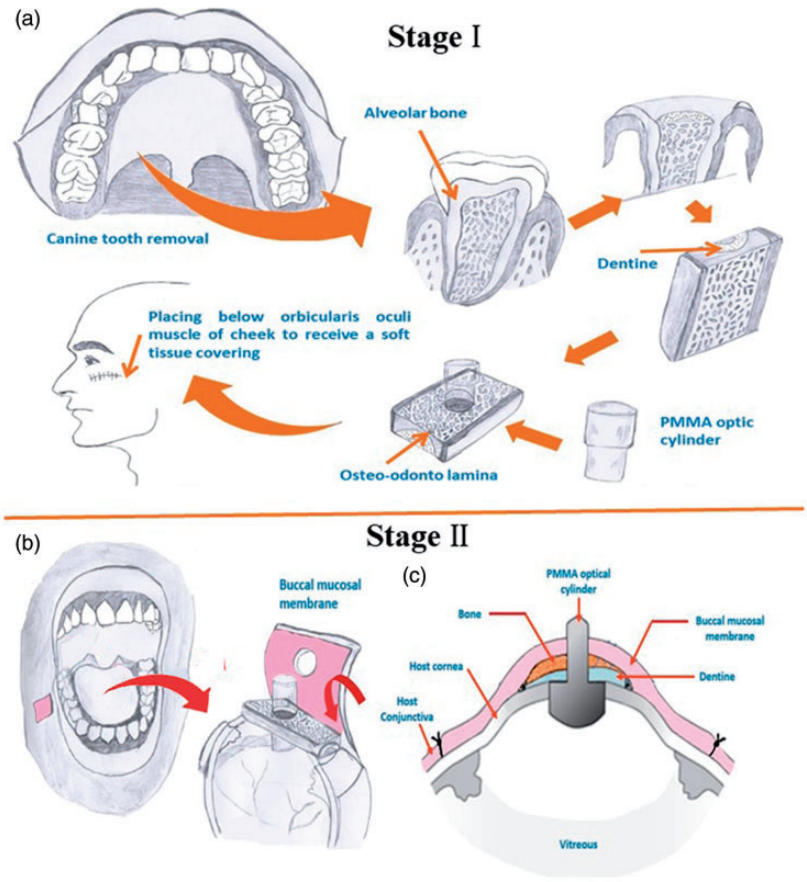

Figure 1. Stepwise illustration of OOKP surgery. (a) the removal of the autologous canine tooth and adjacent bone used to hold an optical PMMA cylinder (Stage I), inserted under the oculi muscle and sutured onto the cornea (Stage II) (b), and (c) schematic representation of cross section of OOKP.

strength or could not support cell adhesion and survival for device integration.

For the past few decades research on polymers for KPro skirt substitutes was conducted using materials ranging from hydrogel and rigid plastics, rubbers and hydrophilic polymers.[48] Water based hydrogels were prepared to facilitate glucose diffusion[49,50] and also surface modified to promote cell adhesion.[51] A number of hydrogel preparation methods were proposed that included synthetic homo- and copolymers, bio-copolymers and interpenetrating networks (IPNs). The first hydrogel KPro from poly(HEMA) (AlphaCor) was prepared by Chirila as a core-skirt model, which was implanted in humans.[13,27] It is a one-piece, soft and flexible device comprises a transparent core (as a central optic) and an opaque porous tissue-integrable skirt. Both components were made of poly(HEMA). This KPro simulated the natural cornea in appearance but was implanted into the corneal lamellae as an intracorneal device with a central opening in the anterior corneal tissue for the exposure of the device to provide a clear visual axis. It is a soft and flexible material liable to mechanical damage and the optic is prone to spoilation over time. The AlphaCor experienced significant complications in cases with ocular surface diseases, herpes infection or severe dry eye.[52] Many of the devices were implanted under surgical principles dissimilar to that of OOKP. Although not adopted for clinical use, the device provided valuable insights into the behaviour of these materials and lead to a better understanding of keratoprosthetic applications.

A number of materials have been examined as synthetic OOKP analogues *in vitro* including polyether ketone and polyethylene,[53] coral skeleton and commercial hydroxyapatite,[54] titanium oxide[55] and graphene,[56] and bio-active glass,[57] although the rationale for the material choice was not always clear. Only Duncker *et al*. have so far reported the outcomes of an acrylate polymeric KPro implanted as a synthetic OOKP replacement in humans.[58] However the material suffered surface spoilation and required surface modification for biointegration. The durability of the OOKP lamina is attributed to the strength and stability of

the alveo-dental laminal tissue.[54] The porosity and hydroxyapatite (HA) richness of the lamina promote its integration within the eye.[59] A synthetic substitute should ideally possess the best properties of the OOKP lamina. It should be biocompatible; promoting tissue integration within the ocular tissue. In addition, the material should have enough minimum physical strength to retain the optic in its centre and sustain the forces created by the blink reflex, normal eye rubbing or other impactful trauma. Although the rigid dental lamina of the OOKP serves all of these purposes, its rigidity can pose difficulties in attachment to the ocular tissue. Therefore, a flexible skirt material with better elastic properties may contribute to improved retention. A similar approach was undertaken by Pintucci using a Dacron fabric. However, bio-integration was not sustained long term.[36]

Among the various biomaterials, hydrogels are highly porous and retain water, which is a biocompatible trait in corneal soft tissue replacement. Since the skirt material is implanted inside the tissues, a hydrogel material can survive because it is protected, and its fluid content is maintained to retain its structural memory and integrity. The composition of network polymer chains and crosslink density are the main factors influencing the mechanical properties of the hydrogel. A mechanically stronger hydrogel might be obtained, however the higher degree of crosslinking reduces the percent elongation of the hydrogels, producing a more brittle structure.[60] In the case of synthetic hydrogels, hydrogels consisting of two separately cross-linked polymer networks have recently attracted a great deal of interest since mechanically stronger gels can be formed consisting of a less cross-linked "second network" within a more strongly cross-linked "first network".[61] The molar ratio of repeat units of the second network to the first network must be >5. However, the tough and brittle hydrogels may not integrate well with the tissues as they do not promote active cell adhesion. These limitations can undermine the usage of hydrogels as KPro substitutes. Hydrogels have significant potential as OOKP skirt materials if their strength and tissue integration properties could be improved. A hydrogel like PEGDA offers the advantage of bio-integration and tuneable implant strength and could address these issues. It has previously been shown that when used as a second network in IPN hydrogels, PEGDA helped significantly in boosting the mechanical performance relative to individual constituent networks while maintaining viability of encapsulated cells for bone[62] and cartilage[63–66] tissue engineering applications.

Numerous studies have documented that the incorporation of nHAp crystals into hydrogels promoted cellular growth and formation of extracellular matrix (ECM) by the colonised cells without causing systemic or local toxicity.[67–70] nHAp was initially used as an osteo-conductivity enhancer for different materials by releasing ions required for bone formation due to its chemical interaction with bone forming cells and the native microenvironment[71,72] and thus providing nucleation sites for cell integration.[62] In previous study we explored the role of nHAp coated polymeric microspheres encapsulated in Interpenetrating network (IPN) hydrogel towards improving the mechanical integrity and osteo-conductive performance in bone tissue engineering-related applications.[62] We observed that, the inclusion of nHAp in an IPN hydrogel resulted in a substantial increase in mechanical strength, alkaline phosphatase activity and calcium deposition. The current work adopts the strategy followed in our previous study and applies it to replacement of bone-dentine laminate during an OOKP procedure in the anterior eye that has not been tested yet. In this work, the use of bioactive nano-crystalline hydroxyapatite particles (nHAp) embedded inside a PEGDA IPN test material has been studied to investigate their effect on cell proliferation and viability. This *in vitro* study was aimed to investigate the use of agarose/PEGDA IPN hydrogel as a synthetic replacement for OOKP lamina.

Materials and methods

Materials

2-Hydroxyethyl agarose, poly(ethylene glycol) diacrylate (PEGDA) (molecular weight 6000 Da) and photo-initiator Irgacure 2959 (I-2959), the poly(lactic-co-glycolic) acid (PLGA) [lactic: glycolic copolymer ratio of 85:15 and MWs (50,000–70,000)] pellets were received from Sigma-Aldrich (Steinheim, Germany). A modified simulated body fluid (mSBF) having ionic concentration similar to human blood plasma was prepared in the laboratory according to the procedure stated by Murphy *et al.*[73] The mSBF solution was kept at pH = 6.8 to prevent homogeneous CaP-phase precipitation.

Cell culture

In minimum essential medium (MEM), a human keratocyte strain LR99F was grown in addition to 10% fetal calf serum (FCS), 1% penicillin/streptomycin and passaged by standard trypsinisation.[74] In Dulbecco's modified eagle medium (DMEM), the fibroblast cell line 3T3 from immortal mouse embryo was normally grown, supplemented by 10% (v/v) FCS at a cell density of 6000 cells/cm^2 and maintained at 37°C at 5% CO_2. Using 0.25% typsin-EDTA solution, cells were passaged every 3 days by standard dispersion

and use for *in vitro* experiments and biochemical assays.

Fabrication PLGA microspheres and coating of nano-hydroxyapatite (nHAp) layer on PLGA surface

A typical water-in-oil-in-water ($W_1/O/W_2$) multiple-emulsion procedure was utilised to fabricate biodegradable PLGA microspheres (Figure 2). Briefly, to prepare a primary W_1/O emulsion, 1 mL 5% (w/v) solution of PLGA in ethyl acetate was combined with 100 µL of distilled water for 30 seconds using a probe sonicator (40 W power). To prepare a secondary $W_1/O/W_2$ emulsion, primary W_1/O was added into a 1 mL of PVA (3–5% v/v) saturated with ethyl acetate and vortexed it for 30 seconds for proper mixing. Under continuous stirring, the resulting secondary emulsion of $W_1/O/W_2$ was decanted into a 200 mL PVA (0.3%) PVA. The stirring was continued for 4–5 hrs at ambient temperature for complete evaporation of the ethyl acetate resulting in solid microsphere formation. The microspheres were filtered out and transferred into a 50 mL falcon tube using a least amount of DI water. A pellet of microsphere was formed by spinning microsphere solution in centrifuge at 4000 rpm for 10 minutes. The microspheres from pellet were washed twice with fresh distilled water and subsequently coated with nHAp by incubating in modified simulated body fluid (mSEB) contains the ionic composition equivalent to human blood plasma and 2-fold higher concentration of Ca & P ions (Figure 2).[75] Briefly, the plain PLGA microspheres were hydrolyzed for 15 min in 0.5 M NaOH to functionalize the surface functionalities and then washed with distilled H_2O. Functionalised microspheres were then incubated in mSBF (pH = 6.8) at 37°C for 7 days, ensuring that the solution was exchanged regularly to preserve sufficient ion concentrations, frozen gradually to −80°C, and freeze-dried. Dried nHAp coated microspheres were then sterilized by exposing them under ultraviolet light overnight.

Synthesis of agarose first network and acellular IPN gels

Agarose solutions having concentrations, 2 and 5% (w/v) in phosphate-buffered saline (PBS) were prepared and sterilised by autoclaving for 30 minutes. The hot agarose solutions approximate 39–40°C were then poured using micro-pipette into circular silicon rubber moulds (5 mm dia × 2 mm height), which are placed in between the microscopic glass plates. These moulds are cooled in refrigerator for 10 mins at 4°C. The solid gels, then equilibrated in PBS for 24 hours.

For making acellular IPN gel, agarose disks were soaked under continuous stirring for 6 hours (4 disks/mL) in 20 and 40%w/v PEGD solution containing 10% w/v photo initiator (Irgacure 2959). These soaked agarose gels containing diffused PEGDA and photoinitiator solution then put in rectangular silicon moulds sandwiched among two microscopic glass slides and photopolymerised by exposing them to uv light (312 nm, 3.0 mW/m^2) (Uvitec, Cambridge, UK) for 5 min on each side. Circular 5 mm disks of IPN gel were then cut using a surgical biopsy punch and placed in PBS for 24 hours. Following formulations were used in this study: 2% w/v agarose gel disks soaked in a 20% w/v PEG-DA solution (2–20 IPN) and 5% w/v agarose gel disks soaked in a 40% w/v PEG-DA solution (5–40 IPN).

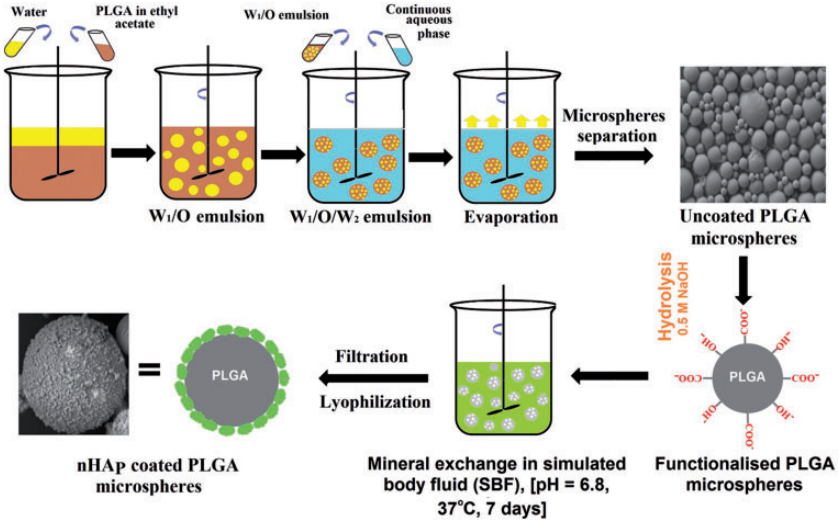

Figure 2. Schematic illustration of a standard $W_1/O/W_2$ double (multiple) emulsion technique for preparation of PLGA microspheres and different stages involved in nano-crystalline hydroxyapatite coating formation on microspheres surface.

Biomineralization and 3T3 mouse embryo fibroblasts/keratocyte encapsulation

Agarose solutions having 3 and 6% concentrations were prepared in PBS and autoclaved for 30 minutes. Using trypsin-ethylenediaminetetraacetic acid (EDTA), cells were detached from tissue-culture flasks and considered as passage 1 (P1). Simultaneously, P1 cells at $1x10^6$ cells/mL in PBS were pooled and re-suspended to start the encapsulation process. When the agarose solution temperature dropped to 39–40°C, the cell suspension in PBS containing 1×10^6 cells/mL and PLGA microspheres coated with nHAp (10 mg/mL) was blended in the liquid agarose in a ratio of 1:2 to reach final concentrations of 2% and 5%. This solution was immediately transferred into circular silicon rubber moulds sandwiched between two microscopic glass slides and refrigerated for 10 minutes at 4°C to prepare the cellular agarose disks. The cell-encapsulated agarose gels then transferred to non-treated tissue culture 24-well plates contain 1 mL culture medium and were incubated at 37°C in an incubator maintained at 5% CO_2. After 24 hours, agarose gel disks encapsulated nHAp-coated microspheres were incubated in sterile solutions of 20 and 50% w/v PEGDA (containing 0.1% Irgacure photointiator) in α-MEM growth medium at 37°C for 6 hrs with under constant stirring. After 6 hours, circular agarose gel disks, containing diffused PEGDA and the photo initiator solution, were then put in sterilised rectangular silicon rubber moulds. To prevent air bubble formation, the extra space in the mould was filled with the leftover PEGDA solution by sterile pipettes from the soak vials. Gel disks were then exposed to UV light ($3.0\,mW/cm^2$) for 5 min on each side for photo-polymerisation. Using a sterile 3–5mm biopsy punch, IPN disks were cut from the rectangular gel slab and cultured for 1 week in growth medium at 37°C with 5% CO_2 in 1 mL of the growth medium.

Equilibrium swelling degree measurement

To remove unreacted PEGDA monomers, acellular IPN gel samples were soaked in excess distilled water for 24 hours to remove unreacted monomers. Swollen IPN gel disks (5 mm dia, $n = 3$) were equilibrated in distilled water for 24 hours. Gels were then transferred to the lab table and blotted with filter paper for complete removal of surface water and weighed. They were then dried to consistent mass under vacuum at 60°C for 48 hours and weighed once more. The degree of swelling Q was determined as the ratio of the equilibrated gel mass to its dry mass.

Mechanical testing

Uniaxial compressive measurements of the swollen equilibrated IPN hydrogels were performed at room temperature using a TA.XT Plus Texture Analyser (from Stable Micro System, UK) with a 5 N load cell ($n = 5$). Mechanical tests were conducted on equilibrated swollen IPN gels in PBS. IPN gel discs (5 mm dia × 2 mm height) were then pressed at a rate of 0.05 mm/s until a fracture occurred. From the initial linear portion on the slope of the curve (<15% strain) the compressive elastic modulus was determined. The compressive modulus from sets of at least 5 samples is stated as mean ± SD values.

Scanning electron microscopy (SEM) and transmission electron microscopy (TEM) analysis

The completely hydrated IPN gel samples were sectioned up to 1 mm slices thick for SEM imaging analysis. Sections of IPN gel samples were then gradually freeze-dried at −80°C and transferred to a Christ freeze dryer at 0.200 mbar vacuum pressure for 18 hours to extract the water from the IPN discs. The freeze-dried IPN slice samples were placed on aluminum stubs and coated using a Quorum (Q150TES) coater with a layer of platinum having 4 nm thickness. The sections were analysed using a field emission scanning electron microscope (FESEM) (Carl Zeiss Microscopy, Germany) at different magnifications at 10 kV. The coating of nHAp on the surface of PLGA microsphere was analysed on a high-resolution transmission electron microscope (TEM) (JEM-2100, Jeol, Japan). For TEM imaging, suspension of nHAp-coated PLGA microspheres in ethanol solution was sprayed on a copper grid with holey carbon film.

Live/dead fluorescence assay

The cell survivability inside the IPN gel with and without bio-mineralised microspheres was assessed at 1 week over 2 D and 3 D IPN gels using a live-dead cytotoxicity kit containing calcein-AM (2 mM) which stain the living cells (Green) and ethidium homodimer-1 (4 mM) which stain the dead cells (Red). Cellular IPN gel discs ($n = 3$) were cut horizontally into 1–2 mm thick slices using a sterile scalpel and incubated for 10 min in Live-Dead staining solution before using confocal microscope. Live/dead images were taken, using a standard confocal microscope (Zeiss LSM-410, Germany) with 488 nm excitation/540 nm emission and 561 nm excitation/585 LP emission filters, Z scans were executed in different areas of representative IPN gels to a resolution depth of 250–300 μm. The percentages of total live/dead cells were quantified with the help of SlideBook mask statistics module (version 5.0).

IL-6 cytokine production

Inflammatory response was determined by measuring production of the pro inflammatory cytokine interleukin IL-6 by 3T3 fibroblasts and keratocytes. For measurement of IL-6 production, both 3T3 fibroblasts and keratocytes were encapsulated at 1x 10^6 cells/mL in plain as well as nHAp incorporated IPN gel discs (diameter = 5 mm and thickness = 2 mm, n = 3). Cells on standard tissue culture plastic (TCP) and on TCP spiked with 10 ng/mL lipopolysaccharide (LPS) were treated as negative and positive controls, respectively. The tissue culture plates were incubated for 5 hours at 37°C. Conditioned media samples (n = 4) were removed at 0, 2, 4, 6, 24 and 48 hrs and stored at −80°C until IL-6 measurement using ELISA method as indicated by the manufacturer using a 1:25 sample dilution in assay diluents (BD Biosciences).

Statistical analysis

All quantifiable data were stated as mean ± standard deviation and statistical significance was determined through a single-factor variance analysis (ANOVA) followed by Tukey's post hoc analysis. Analysis was done using the statistical software package SPSS 17.0. P values below 0.05 were defined statistically significant.

Results

Characterisation of plain and nHAp-coated PLGA microspheres by SEM, TEM and EDX

The surface morphologies of the uncoated and nHAp-coated PLGA microspheres were studied by field emission scanning electron microscopy (FESEM, JSM-6340F, Japan) at 3 kV (Figure 3). The SEM analysis shows uniform PLGA microspheres (size range is 2–50 μm) with a smooth surface (Figure 3(a)). SEM (Figure 3(a) and (b)) and TEM images (Figure 3(c) and (d)) showed continuous deposition of the nHAp mineral film, with a plate-like nanostructure, on the surface of the microsphere. Energy-dispersive X-ray spectroscopy (EDX) confirmed the existence of calcium (Ca), phosphorus (P), carbon and oxygen peaks (Figure 3(e)) related with the PLGA polymer. The average Ca/P ratio is 2.3, which is within biological apatite range.[76]

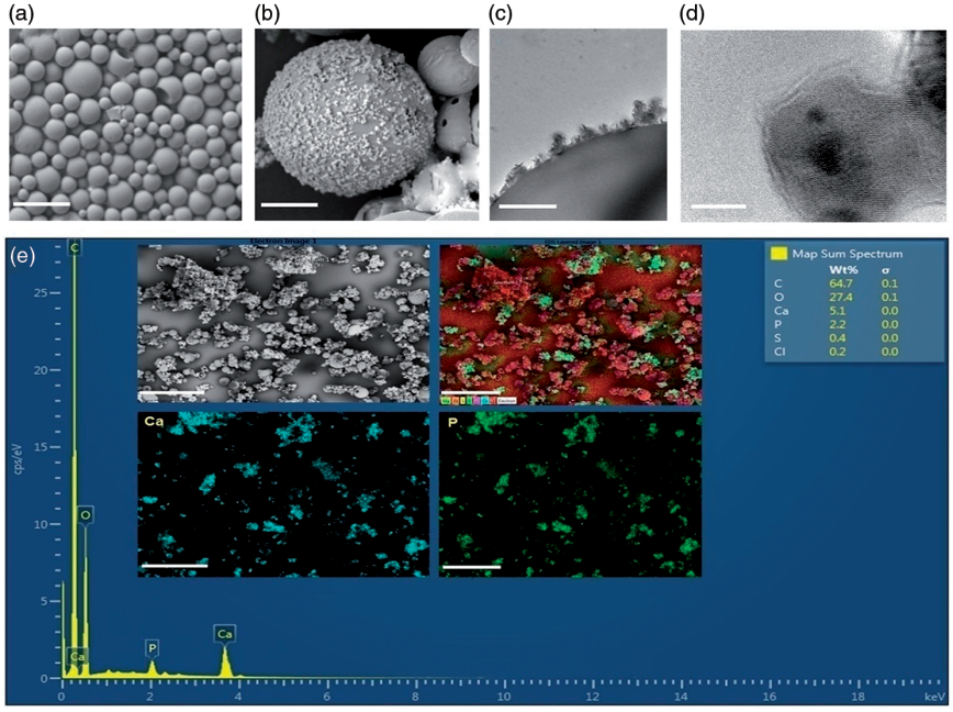

Figure 3. SEM, TEM and EDX analysis results showing the calcium phosphate mineral coating on PLGA microspheres. (a) SEM micrograph showing uncoated microspheres, scale bar = 100 μm, (b) continuous nHAp mineral deposition on microsphere surface, scale bar = 2 μm, (c) TEM image showing continuous HAp crystal coating on PLGA microsphere, Scale bar = 1 μm, (d) TEM images displaying the nanoscale nHAp crystal structures, scale bar = 5 nm and (e) EDX spectra showing Ca and P peaks confirming nano-hydroxyapatite coating on PLGA microspheres surfaces.

The characterization of plain and biomineralised IPN hydrogels

The plain agarose-PEGDA IPN gels were synthesized via a 2-step synthesis method: initially brittle natural polymer gel network was synthesised (first step) and followed by the preparation of a stronger and more ductile synthetic polymer network within the first using photo-polymerisation (second step). The biomineralised IPN gels were synthesised using the same method as above, as shown in Figure 4. Biomineralised cellular IPN was synthesized in this study incorporating nHAp coated PLGA microspheres (10 mg/mL) along with cell having $1x10^6$ cells/mL seeding density. The SEM images were acquired to investigate the microstructure of freshly prepared freeze-dried gels and are shown in Figure 5. Morphological analysis of acellular agarose and IPN using SEM images displayed pore structures that are homogeneously interconnected (Figure 5(a) and (b)), while Figure 5(c) and (d) shows the consistent dissemination of incorporated biomineralised PLGA microspheres at the IPN gel surface and inside of IPN gel, respectively. This confirms the existence of a highly interconnected macro-porous gel network with very well-ordered architecture and well-defined pores.

Macroscopic images of the equilibrated gel samples with all the formulations and their response to compression are shown in Figure 6(a). The swelling degrees of plain (2–20, 2–30, 5–30, 5–40 IPN) and nHAp encapsulated (2–20 IPN + nHAp and 5–40 IPN + nHAp) gels are shown in Figure 6(b). There were significant differences in the swelling degree within groups, and concentration of PEGDA was found the most imperative contributing feature. Increases in concentration of PEGDA resulted decreasing in swelling, and trends usually displayed an inverse connection between PEG-DA concentration and the compressive modulus. 5–30 and 5–40 IPN gels displayed a 30% and 36% decrease in swelling degrees relative to 2–20 IPN, respectively, while the presence of bio-mineralised microspheres resulted in a 38% decrease in the swelling degree relative to the plain/un-coated IPN hydrogel (2–20 IPN) ($P = <0.05$, $n = 5$), but this decrease in swelling degree was not statistically significant compare to the 5–30% and 5–40% IPN formulations. 2–20 IPN + nHAp gel reported a 5% reduction in swelling degree, but this reduction was not statistically significant compared to 2–20 IPN.

Mechanical compression testing was performed using the mechanical texture analyser equipped with a 5 N load cell to assess the mechanical properties of plain and biomineralised IPN gels. Figure 6(c) shows maximum stress and the strain percentage of all 6 IPN gel formulations. Until a stress level of 3 to 3.5 MPa was reached certain formulations did not fracture. Some formulations such as, 5–40 IPN, 2–40 IPN +nHAp and 5–40 IPN + nHAp, did not fracture with 100% compression at all. Figure 6(c), displays the typical stress–strain curves of IPN hydrogels groups with and without nHAp coated microspheres in it. For all formulations, the compressive moduli were determined from the slope of the initial (<20% strain) linear stress-strain curves. Higher concentrations of agarose and PEGDA can result in increased crosslinking density, resulting in increased hydrogel stiffness. Increase in PEGDA concentrations in 2–40 IPN gel increased compressive modulus by 4-fold (11,099 Pa) relative to 2–20 IPN gel (2730 Pa), while increase in both agarose

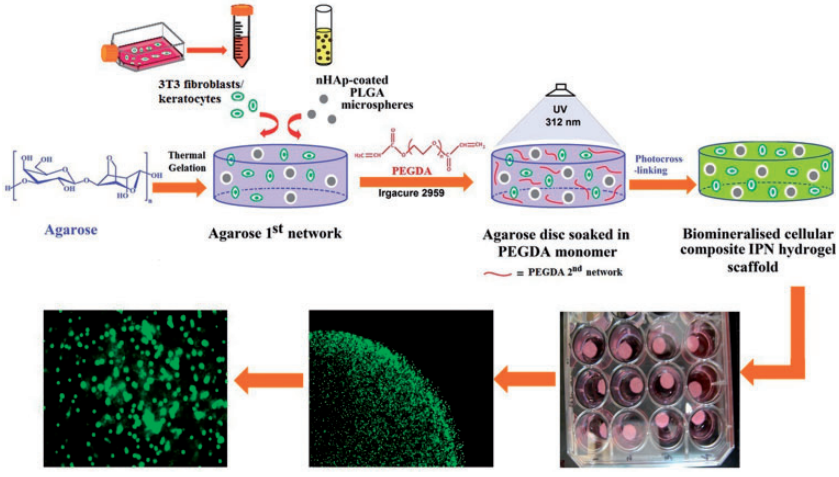

Figure 4. Schematic illustration displaying the preparation of cellular agarose/PEGDA IPN gel containing biomineralised microspheres made from PLGA polymer. During the synthesis of the first 2-hydroxyethyl agarose network, nHAp, a natural and major mineral component of bone, was encapsulated through nHApcoated PLGA microspheres inside the hydrogel.

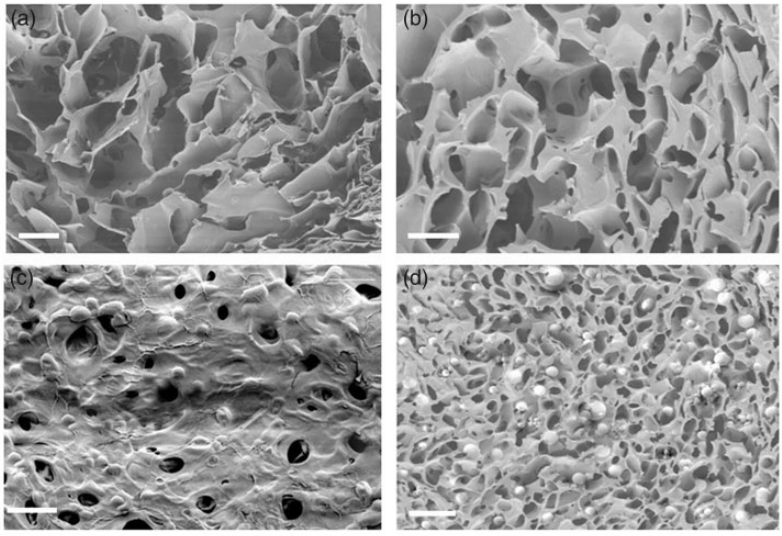

Figure 5. Representative SEM micrographs showing internal porous structure of (a) agarose and (b) IPN gel and consistently dispersed nHAp-coated PLGA microspheres at (c) surface (d) inside the IPN gel (scale bar = 100 μm).

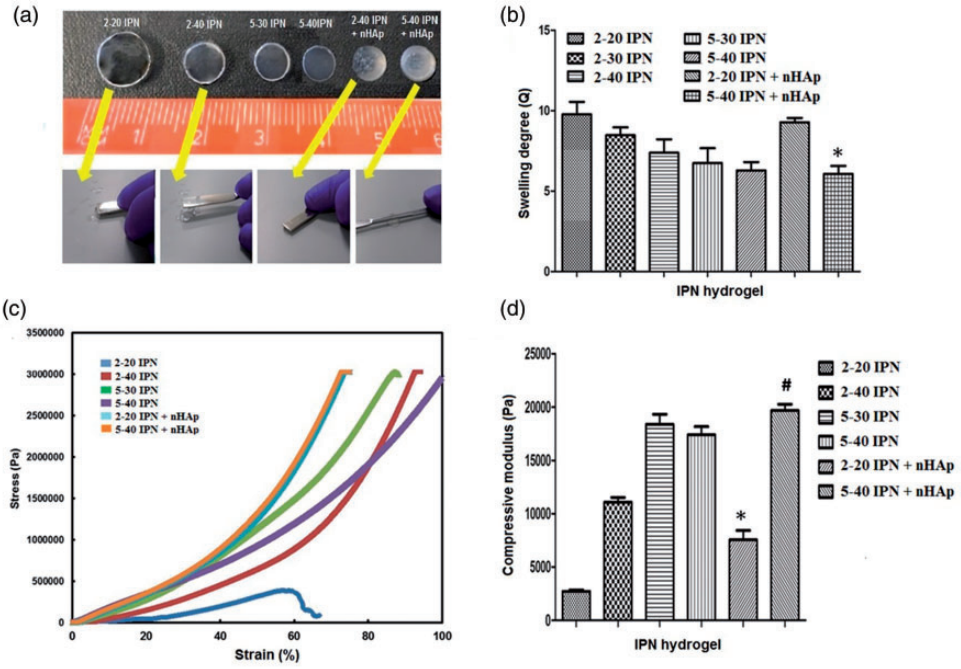

Figure 6. Mechanical and swelling properties of IPN hydrogels. (a) macroscopic equilibrated gels with all formulations and their mechanical behaviour during compression by spatula, (b) swelling degrees, (c) typical stress-strain curves of plain and bio-mineralised IPN hydrogels, and (d) compressive modulus of IPNs produced with different agarose-PEGDA formulations. The samples were positioned at the centre, among the texture analyser compression plates and pressed at a steady rate of 0·05 mm/s. * and # indicates statistically significant differences compared to the respective plain formulations ($p < 0.05$ and $n = 5$).

and PEGDA it increases by 6-fold (18,393 Pa) ($p < 0.05$, $n = 5$). Furthermore, the IPN gel containing the encapsulated bio-mineralised (nHAp-coated) microspheres displayed enhancement in the amount of stress that the gels could endure until a fracture (Figure 6(c)). The presence of bio-mineralised microspheres in the IPN hydrogel 2–20 IPN + nHAp and 5–40 IPN + nHAp resulted in an increase in compressive modules of 2·8 (7550 Pa) and 7.2-fold (19,680 Pa), respectively, compared to IPN hydrogels containing no biomineralized microspheres (2–20 IPN) (2730 Pa) (Figure 6(d)).

2D and 3D biomineralized IPN hydrogel microenvironments for 3T3 fibroblasts and keratocytes

IPN gels with different agarose (2 and 5 w/v %) and PEGDA (20 and 40 w/v %) concentrations, with and without nHAp coated PLGA microspheres have been synthesized aseptically in 96 well plates for 2 D and 3 D 3T3 fibroblast and keratocyte cultures using the UV photopolymerization technique as described earlier in methods section. Schematic representation of 2 D and 3 D IPN gel environments from the context of cultured cells is shown in Figure 7. It is evident from Figure 7, that cell shape and morphology were different between 2 D culture plate (Figure 7(a)), 2 D hydrogel surface (Figure 7(b)) and 3 D cell growth conditions (Figure 7(c)). Cells grown on the 2 D hydrogel surface (Figure 7(b)) experienced less rigidity when compared to traditional cell culture plate, but they cannot completely mimic the native tissue microenvironment, which a 3 D microenvironment (Figure 7(e) and (f)) may be able to provide.

Cell survivability

After 3T3 fibroblasts and keratocyte encapsulation in 2 D and 3 D IPN cultures, a live/dead fluorescent assay was performed to assess cell viability at the 1-week time point. Comparison of 2 D and 3 D cultured cells using IPN gels using live/dead (calcein AM and ethidium homodimer dye) cell staining showed that most of the encapsulated cells remained viable (fluorescent green) over a 7-day culture period in composite IPN hydrogels containing mineral coated microspheres (Figures 8(c), (d) and 9(c), (d)). To study cell viability during the encapsulation process, a live/dead assay was carried out on both 2 D and 3 D matrices at 1 week in culture. 3T3 fibroblasts and keratocytes at a density of 10 million cells/mL and four different IPN gel formulations including nHAp coated microspheres were used in this study. Data from the mask statistics analysis showed that, over 80% of the 3T3s and keratocyte cells were viable for up to 1 week in 2 D hydrogel cultures (Figures 8(g) and 9(g)). Moreover, comparison of changes in viability over 1 week indicated that, viability of 3T3 fibroblasts improved in 2 D gels from 86.3% to 90.3% (an increase of 4.6%) and 82.3% to 89.3% (an increase 8.5%, $p < 0.05$) in 2–20 IPN + nHAp and 5–40 IPN + nHAp, relative to their corresponding plain formulations of 2–20 and 5–40 IPN, respectively (Figure 8 (g)). The 2 D keratocyte viability increased from 78% to 87% (an increase of 11.5%) and from 78% to 81.3% (an increase 4.2%, $p < 0.05$) in 2–20 IPN + nHAp and 5–40 IPN + nHAp samples, relative to their plain formulations of 2–20 and 5–40 IPN samples, respectively (Figure 9(g)).

Interestingly, encapsulated 3T3 fibroblasts and keratocytes retained their spherical morphology inside the hydrogel construct (Figure 10(a) to (h)). Further finding was that encapsulated 3T3 fibroblasts (Figure 10(a) and (b) and keratocytes (Figure 10(e) and (f)) were dispersed uniformly throughout the nHAp free IPN hydrogel matrix. Whereas, in the presence of mineral-coated PLGA microspheres the fibroblasts (Figure 10

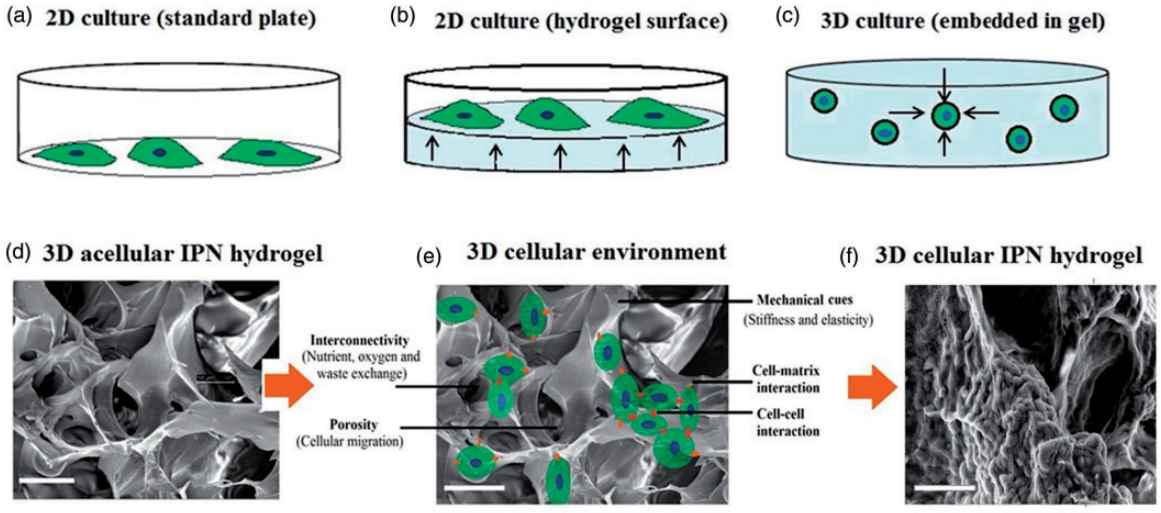

Figure 7. Schematic representation of 2 D and 3 D cell microenvironments. Cells were cultured on 2 D tissue culture plastic (a), or 2 D hydrogel surface (b) or embedded in 3 D hydrogel (c). Only a portion of a cell's surface comes in contact with the plastic or gel surface. Cells encapsulated by a hydrogel that provides 3 D microenvironment and matrix for the cell's entire surface to interact (e, f), Scale bar = 50 μm. Keratocytes in 2 D culture adopted spread morphology while in a 3 D microenvironment they adopted a spherical morphology as hydrogel network essentially acted as a physical restraint that retained the cell's spherical morphology.

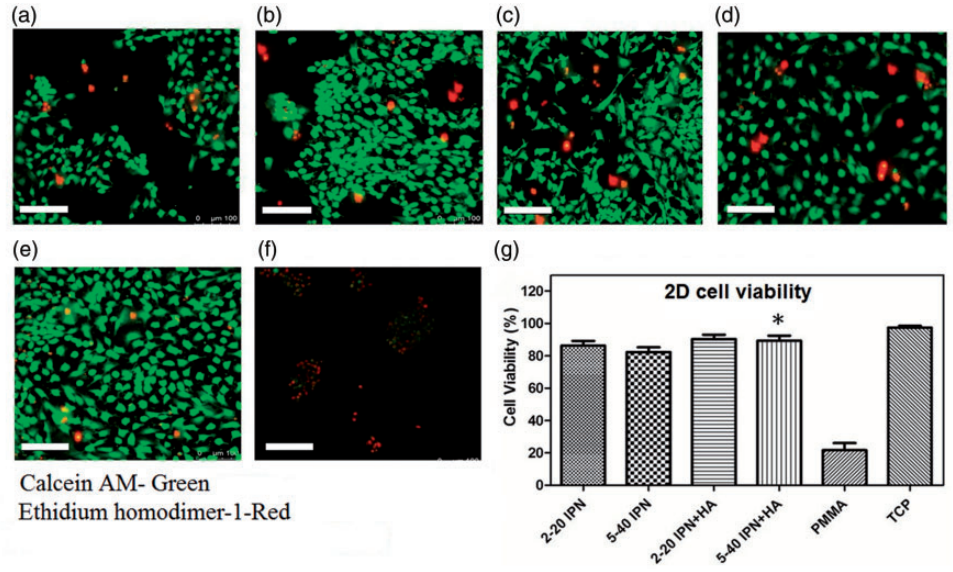

Figure 8. Confocal laser scanning microscopy (CLSM) live/dead images of 2 D cultured 3T3 fibroblasts on (a) 2–20 IPN, (b) 5–40 IPN, (c) 2–20 IPN + nHAp, (d) 5–40 IPN + nHAp, (e) positive control TCP, and (f) negative control PMMA at day 7, Scale bar = 100 μm. (g) Percentage viability of encapsulated 3T3 fibroblasts evaluated by image analysis mask statistics tool. In each group, multiple confocal Z-scan series were performed on one representative sample. *values indicate significant differences ($p < 0.05$, $n = 3$, mean ± SD).

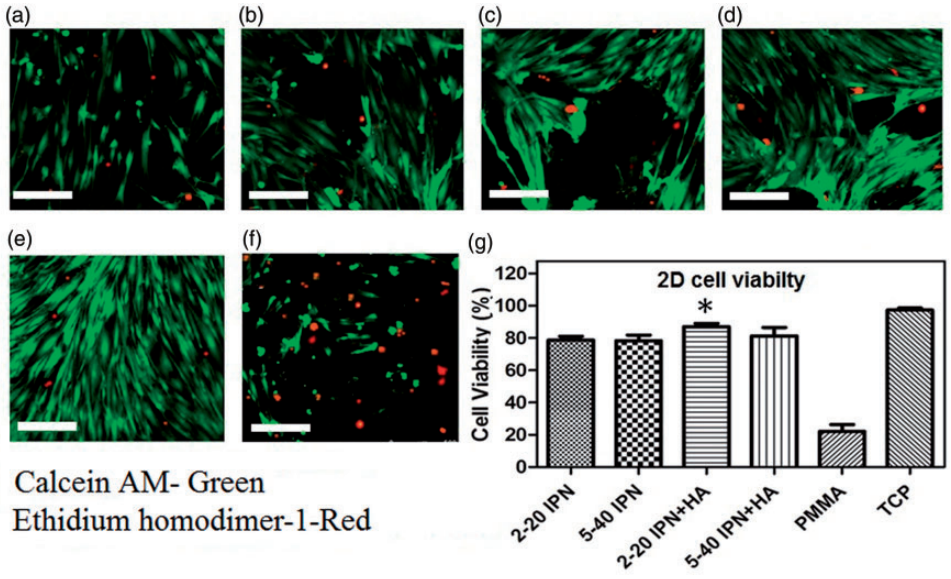

Figure 9. Confocal microscope live/dead images of 2 D cultured keratocytes on (a) 2–20 IPN, (b) 5–40 IPN, (c) 2–20 IPN + nHAp, (d) 5–40 IPN + nHAp, (e) positive control TCP, and (f) negative control PMMA at day 7, Scale bar = 100 μm. (g) Percentage viability of encapsulated keratocytes determined by mask statistics image analysis tool. In each group, multiple confocal Z-scan series were performed on one representative sample. *values indicates significant differences ($p < 0.05$, $n = 3$, mean ± SD).

(c) and (d)) and keratocytes (Figure 10(g) and (h)) appeared in clusters or aggregates around the nHAp rich areas in the hydrogel. This suggested enhanced adhesion, migration and proliferation of cells on the PLGA surface and the positive influence of nHAp on viable cell growth. The viability of both 3T3 fibroblasts and keratocytes in 3 D IPN hydrogels culture was high, but less than optimal in the absence of PLGA microspheres coated with nHAp. However, percentage cell viability increased in the presence of nHAp from 70% to 79.6% (an increase of 13.7%) and 66.3% to 75.6% (an increase of 14%, $p < 0.05$) in 2–20 IPN + nHAp and 5–40 IPN + nHAp, relative to their plain 2–20 and 5–40 IPN formulations, respectively

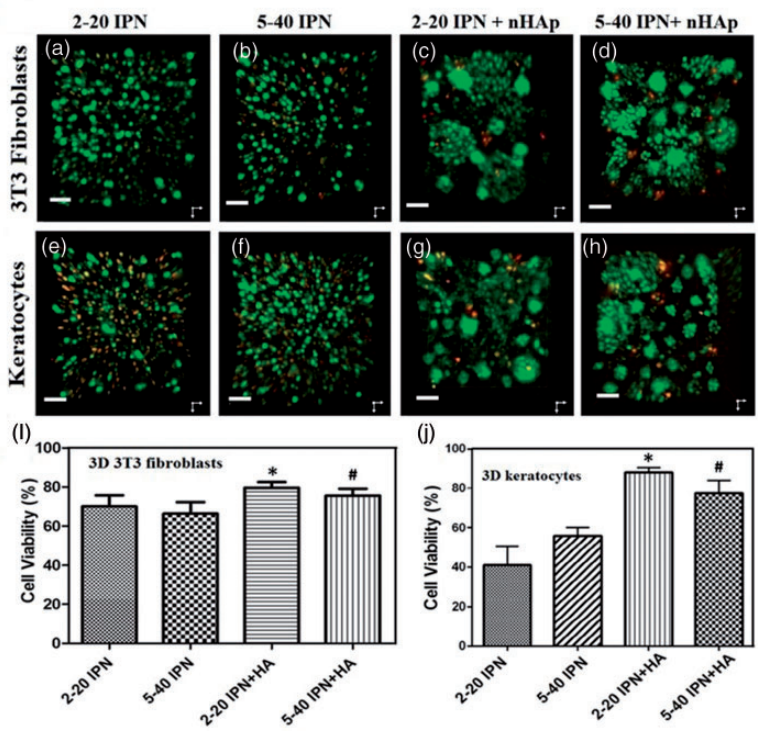

Figure 10. Three-dimensional projections of spinning disc confocal microscope live/dead images of 3T3 fibroblasts on (a) 2–20 IPN, (b) 5–40 IPN, (c) 2–20 IPN + nHAp, and (d) 5–40 IPN + nHAp, while keratocytes on (e) 2–20 IPN, (f) 5–40 IPN, (g) 2–20 IPN + nHAp, and (h) 5–40 IPN + nHAp at day 7 (Scale bar = 50 μm). In presence of nHAp cells tends to form clusters/aggregates around the PLGA microspheres surfaces. Cell viability percentage of encapsulated (i) 3T3 fibroblasts and (j) keratocytes by image analysis masks statistics tool. In each group several confocal Z-scans were performed on a representative sample [mean ± SD]. * and # values indicate statistically significant differences in comparison with their corresponding plain formulations ($p < 0.05$ and $n = 3$).

(Figure 10(i)). In the case of keratocytes cell viability increased 2.1 (40% to 84.4%) and 1.3-fold (56% to 78%) in 2–20 IPN + nHAp and 5–40 IPN + nHAp, relative to their plain formulations 2–20 and 5–40 IPN formulations, respectively (Figure 10(j)).

Cytokine production

Supernatant media samples collected at 2, 4, 6, 24 and 48 hrs from the wells of cell encapsulated IPN gels were found to contain IL-6 after 5 hrs of incubation. The different fibroblast types showed a different cytokine expression profile on contact with the IPN gels (Figure 11(a) and (b)). The 3T3 fibroblasts didn't express detectable IL-6 until the 4 hr time point and IL6 expression, then increased over time until the final 48 hr time point (Figure 11(a)). The keratocytes expressed IL-6 earlier, at the 2 hr time point, except in the 5–40 IPN+ nHAp sample (Figure 11(b)). Expression peaked at 6 hours and then declined at the later time points. This was in contrast to the cells exposed to LPS where IL-6 expression occurred at the 2 hr time point and continued to rise to significantly greater levels at the 48 hrs final time point than in the

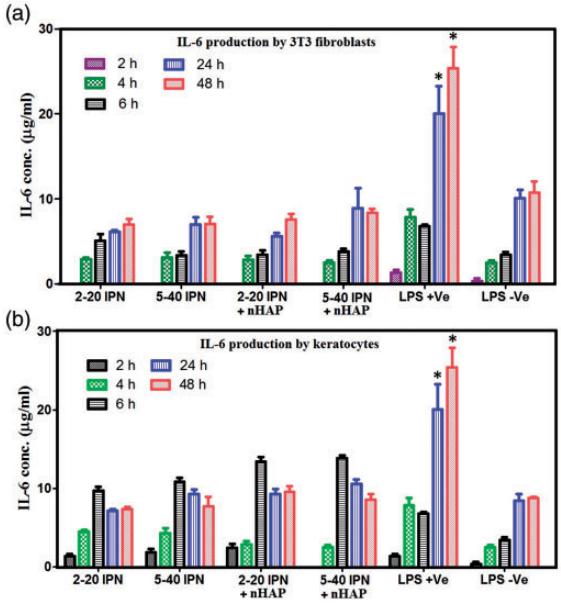

Figure 11. Measurement of cytokine IL-6 produced by (a) 3T3 fibroblasts and (b) keratocytes in contact with plain as well as nHAp–coated PLGA microspheres incorporated IPN gels. *values indicate significant differences ($p < 0.05$, $n = 3$, mean ± SD).

IPN gel samples in both cell types. IL-6 concentration increased over time in the 3T3 cell supernatant for all samples but peaked at the 6-hour time point in the keratocyte IPN samples. No significant difference was found in the production of IL-6 content in the plain and nHAp incorporated IPN gels compared to the negative control group and each other.

Discussion

Development of an implantable synthetic OOKP analogue would transform OOKP surgery and broaden the use of the procedure worldwide. An artificial lamina instead of the tooth offers several advantages by reducing surgical morbidity and improving device design. It also provides the opportunity to produce custom designed KPro skirts and improve the design of the optic, potentially enhancing the visual field.

Alveo-dental lamina has specific features that make it integrate well within the eye. The dentine portion, which rests on the globe directly, integrates well and, as the strongest tissue, it stays longer and provides a stable platform, while the alveolar portion above the dentine layer of the lamina helps to establish a vascular connection with the buccal mucosa. Being a rigid and mechanically strong tissue resting over the surface of the globe, it copes well with the physical stress of eye movement and blinking. Moreover, being an epicorneal device, the bulk of this biological skirt is adherent to the globe and is not in direct exposure to the corrosive action of the aqueous humour. The external part of the skirt is protected by a tough mucosal tissue. This arrangement offers a biologically sustainable environment for a skeletal tissue graft in an abnormal location such as the eye. The same principle can be harnessed with suitable biomaterials. Pintucci KPro has a Dacron skirt with a rigid optic and is implanted under the same principles as the OOKP including its pre-implantation into the sub muscular pouch for vascularisation before the transfer to the eye.[25] However, this device is not widely available and did not show promising success.[77]

Creation of hydrogels to match the mechanical strength and HA rich microenvironment of the OOKP lamina is a challenge. Recent studies have shown that hydrogels can be customised for guided tissue ingrowth by influencing the cellular interactions.[78] Hitherto, the traditional methods of fabrication provide hydrogels with low mechanical strength and as such they fail to meet the requirements for hard tissue applications.[79] However, by employing hybrid networks and modulating the concentrations of the polymeric substance, the mechanical stiffness of the hydrogels can be fine-tuned.[80] Synthetic hydrogels are of interest for a number of biomedical applications because their mechanical strength, porosity and water content can be tuned to meet the requirements of a specific tissue. The double network IPN hydrogels developed in this study are particularly suited to replace the OOKP lamina since they are biocompatible, non-inflammatory, have tuneable porosity and mechanical strength, can support long-term cell survival, can be fabricated with the required morphology, have high stability and durability in the swollen state and for storage. The properties of this novel IPN skirt were assessed in our current and previous work *in vitro*,[62] in order to optimise these materials for dentine tooth substitution within the OOKP surgical procedure. Previously, the authors explored agarose-PEGDA IPN hydrogels containing nHAp that exhibited cytocompatibility with the production of an ECM similar to bone matrix, which also has enhanced the mechanical properties of the IPN compared to the base networks.[62]

Biological tissues with natural calcification such as bones and teeth contain mineral composition similar to HAp. Resorption studies on commercial bone substitutes and corals indicate that HAp alone is unstable and not appropriate as a KPro skirt material.[54] Therefore, HAp should be integrated with stable and accommodative biomaterials. In current work, we investigated a two-step system to integrate nHAp-coated polymeric microspheres within the stable agarose-PEGDA gel framework. This approach has proven that a stable polymer system can be generated.

In this two-step process, PLGA microspheres were prepared using a $W_1/O/W_2$ multiple-emulsion technique and inorganic nHAp was coated over the surface of microspheres by incubating in an aqueous solution, modified simulated body fluid (mSBF), having an ionic composition of blood plasma but in a doubled concentration of Ca and P.[81] Investigation with SEM, EDX and TEM have shown the development of HAp layer on the surface of PLGA microspheres. The average Ca/P ratio of the formed nHAp layer was found to be 2:3 as detected in EDX analysis that is near to the bone composition.[76,82] It is encouraging that the morphology and mineral constitution of the nHAp coating on PLGA microspheres was comparable to that of the bones, which will promote colonisation of the cells, their proliferation and differentiation. Additionally, with our method selective instillation of the nHAp laden microspheres is possible into the different parts of the hydrogels and the density of the mineral deposition can be controlled for desired level of tissue integration of the material *in vivo*.

The synthetic OOKP skirt should be strong and has the ability to retain the optical segment in-vivo and bear the physical forces of continuous blinking and saccadic eye movements. Research on tissue engineering with combined network hydrogels made from

Agarose and PEGDA polymers have displayed enhanced mechanical properties against the individual networks while retaining their properties to support the growth of cartilage cells[63,64] and osteocytes.[62] The physical strength of the agarose-PEGDA hydrogel IPN was improved in this study by increasing the concentrations of both the polymers and was further increased by the incorporation of the hydroxyapatite. For the purpose of the OOKP skirt a high strength hydrogel is required, which is achieved by these novel techniques. A synthetic substitute should ideally possess the best properties of the OOKP lamina. It should be biocompatible and promote integration with the surrounding ocular tissue. Bio-integration of an implant ensues by the orchestration of direct structural, physical and biochemical interactions between the cells and living tissue of the host and the biomaterial surface.[83] The material should have enough physical strength to retain the optic in its centre and sustain the forces of eyelid blinking and trauma related to eye rubbing or other forces acting on the eye. The poor bio-integration between the optic material (bioinert hydrophobic and texture-less surface) and the biological skirt material is a critical inadequacy of core-skirt KPros,[84–89] resulting in poor bonding which has led to various complications including extrusion of the optical cylinder.[84,85,87,89] In addition to its ability to bond with the non-porous and rigid optical cylinder, mechanical integrity is a significant aspect of the intended skirt polymer. The polymer should have enough mechanical strength to hold the optic in place and to be placed in the eye. This polymer based IPN skirt prepared in this work offers the advantage that it can be moulded to fit the curved globular surface of the eye without causing its compression. However, it needs further *in vitro* experiments and *in vivo* testing.

A 5% w/v concentration of the agarose was the highest to allow viable cell encapsulation as it tends to gelate at temperatures higher than 37°C. The 2% w/v agarose is the commonly used concentration of agarose for IPN development in tissue engineering studies. We observed that the compressive modulus of the IPNs containing agarose-5% was significantly higher ($p < 0.05$) than the IPNs with agaros-2%. Similarly, mechanical strengths were higher in gels with high concentrations of PEGDA (30%, 40%) than the gels with low concentration of the PEGDA (20%). Incorporation of the nHAp layered PLGA microspheres has increased the compressive moduli of the gel discs compared to the gels without the incorporation in all the IPN formulations with different concentrations of the polymers.

The microenvironment suitable for solute transport and oxygen diffusion depends on the gel porosity, density of cross-linkage among the polymer chains and the volume fraction in the swollen state of the multi-network polymers. The mesh size and swellability of the IPNs made with 5% agarose were significantly low compared to the IPNs with 2% agarose and single PEGDA networks ($p < 0.05$). Likewise, higher concentration of PEGDA molecules resulted in smaller mesh sizes and lower degree of swelling but provided higher mechanical strength. An increase in polymer concentration resulted in increased network stiffness due to increased crosslinking density. Consequently, the gels develop more resistance to deformation with load application. However, the elastic modulus has demonstrated an inverse relationship with the degree of swelling, which is in line with the rubber elastic theory.

The architecture of the IPN gels as studied with SEM revealed a highly ordered and interconnected porosity with distinct pore boundaries. A thin "shell" of polymer covered most of the surface, while the pores were strongly interconnected within the hydrogel, enabling cell migration and proliferation. Overall, the networks were microporous with an average size ranging between 50–200 μm. This maximises exposure of the nHAp surface which is favourable for 3T3 fibroblasts and keratocyte adhesion, migration, proliferation and differentiation. Previously, it has been shown that living cells continue to proliferate over time (indicated by an increase in DNA content) in this type of interconnected porous IPN hydrogels when cultured for 3 weeks.[65]

Various types of cells were studied in 3 D microenvironments to investigate the techniques for improved cell performance and long-term viability, to our knowledge, there are no reports on the encapsulation of 3T3 fibroblasts and keratocytes in IPN gels and their direct comparison with 2 D cell culture. More than 75% of the cells were alive after a week of seeding in both the surface 2 D and deep 3 D cultures when nHAp loaded PLGA microspheres were employed. Moreover, the survivability of the cells in 3 D hydrogel culture proved the sufficient permeability of the gels to transport oxygen and nutrients to the cells. The interactions among the cells and between the cells and ECM are possible in 3 D cultures, unlike the surface 2 D cultures on the hydrogels. Interestingly, we observed that the cells have gathered at the locations of nHAp aggregates on the surface as well as inside the hydrogels, which can be exploited by selective instillation of these substrates at the required locations for a custom-built KPro skirt. The mineralised microspheres also facilitated improved cell viability, apart from encouraging cell migration, by acting as the nucleation sites for Ca and P secreted by the cells.

The Inflammatory propensity of the IPN materials with and without nHAp loaded PLGA microspheres

was assessed by studying the amount of IL-6 secretion by both 3T3 fibroblasts and keratocytes. The IL-6 secretary response of both fibroblast and keratocytes cultured on all nHAp coated and uncoated hydrogel preparations was less than or equal to that of the response from cells in contact with the tissue culture plate. It denotes that the PEGDA-agarose IPN combination and the nHAp coated PLGA microspheres do not incite any inflammatory reaction on the cell cultures. This is particularly relevant to the KPro skirts, which are implanted in eyes prone to inflammation.

Conclusions

Hydrogel IPNs have historically been used in soft tissue engineering applications due to their low mechanical strength and lack of adhesion to the cells. In this study, nHAp incorporation into the hydrogel was performed to create a microenvironment like that of alveodental complex in OOKP lamina. High strength double network polymers were created by employing PEGDA and agarose in higher concentrations and by embedding nHAp coated PLGA microspheres into the gels. This method has greatly improved the compressive modulus and mechanical strength of the hydrogels. Both 2 D and 3 D cultures were undertaken on 3T3 fibroblasts and human keratocytes by cell encapsulation technique during the gel preparation. The cell viability was unaffected by increasing the polymer concentrations. This approach provides a cell instructive 3 D microenvironment by creating IPN hydrogels of varying stiffness in the range of 2.7–19.6 kPa and by altering agarose and PEGDA networks. The cell growth and viability were increased by adding nHAp into the hydrogel formulations. We have also demonstrated that the majority of cells (>80%) were viable at 1-week post-encapsulation in a 3 D microenvironment containing bone-like mineral coated PLGA microspheres. Moreover, IL-6 production by cells in the presence of IPN materials was not different to the control group demonstrating the non-inflammatory nature of the plain and composite IPN gels and suggesting that these materials could be potential candidates for replacing bone-dentine tissue during OOKP surgery. The findings of this study suggest that PEGDA-agarose based IPN can provide a hydrogel with physico-chemical and mechanical properties and microenvironment that can be tailored to mimic the properties of OOKP lamina.

Declaration of conflicting interests

The author(s) declared no potential conflicts of interest with respect to the research, authorship, and/or publication of this article.

Funding

The author(s) received no financial support for the research, authorship, and/or publication of this article.

ORCID iDs

Ganesh Ingavle https://orcid.org/0000-0001-5044-2075
Susan Sandeman https://orcid.org/0000-0001-8367-2758

Supplemental material

Supplemental material for this article is available online.

References

1. Meek KM and Knupp C. Corneal structure and transparency. *Prog Retin Eye Res* 2015; 49: 1–16.
2. Burton MJ. Prevention, treatment and rehabilitation. *Community Eye Health* 2009; 22: 33–35.
3. Torricelli AA, Santhanam A, Wu J, et al. The corneal fibrosis response to epithelial-stromal injury. *Exp Eye Res* 2016; 142: 110–118.
4. Oliva MS, Schottman T and Gulati M. Turning the tide of corneal blindness. *Indian J Ophthalmol* 2012; 60: 423–427.
5. Yu T, Rajendran V, Griffith M, et al. High-risk corneal allografts: a therapeutic challenge. *World J Transplant* 2016; 6: 10–27.
6. Moffatt SL, Cartwright VA and Stumpf TH. Centennial review of corneal transplantation. *Clin Exp Ophthalmol* 2005; 33: 642–657.
7. Mannis MJ, Mannis AA and Albert DM. *Corneal transplantation: a history in profiles*. Oostende, Belgium: J.P. Wayenborgh, 1999.
8. Pellier de Quengsy G. *Précis au cours d'operations sur la chirurgie des yeux*. Paris, France: Didot, 1789.
9. Crawford AZ, Patel DV and McGhee C. A brief history of corneal transplantation: from ancient to modern. *Oman J Ophthalmol* 2013; 6: S12–7.
10. Alio JL, Abdelghany AA, Abu-Mustafa SK and Zein G. A new epidescemetic keratoprosthesis: pilot investigation and proof of concept of a new alternative solution for corneal blindness. *Br J Ophthalmol* 2015; 99: 1483–1487.
11. Gomaa A, Comyn O and Liu C. Keratoprostheses in clinical practice - a review. *Clin Exp Ophthalmol* 2010; 38: 211–224.
12. Barber JC. *Design of a retainable keratoprosthesis: history, design and evaluation in cats*. 1st ed. Bloomington, USA: Author House, 2011.
13. Chirila TV, Hicks CR, Dalton PD, et al. Artificial cornea. *Progress in Polymer Science* 1998; 23: 447–473.
14. Caldwell DR. The soft keratoprosthesis. *Trans Am Ophthalmol Soc* 1997; 95: 751–802.
15. Ruedemann AD Jr. Silicone keratoprosthesis. *Trans Am Ophthalmol Soc* 1974; 72: 329–360.
16. Polack FM. Clinical results with a ceramic keratoprosthesis. *Cornea* 1983; 2: 185–196.
17. Stone W and Herbert E. Experimental study of plastic materials as replacement for the cornea. *Am J Ophthalmol* 1953; 36: 168–173.

18. Stone W Jr. Alloplasty in surgery of the eye. *N Engl J Med* 1958; 258: 596–602.
19. Cardona H. Mushroom transcorneal keratoprosthesis (bolt and nut). *Am J Ophthalmol* 1969; 68: 604–612.
20. Choyce DP. Evolution of choyce 2-piece multistage perforating keratoprosthesis technique: 1967–1978. *Ann Ophthalmol* 1980; 12: 740–743.
21. Cardona H. Prosthokeratoplasty. *Cornea* 1983; 2: 179–183.
22. Singh D. Keratoprosthesis. *Indian J Ophthalmol* 1984; 32: 405–407.
23. Dohlman CH, Schneider HA and Doane MG. Prosthokeratoplasty. *Am J Ophthalmol* 1974; 77: 694–670.
24. Girard LJ. Keratoprosthesis. *Cornea* 1983; 2: 207–224.
25. Pintucci S, Pintucci F, Cecconi M, et al. New dacron tissue colonisable keratoprosthesis: clinical experience. *Br J Ophthalmol* 1995; 79: 825–829.
26. Pintucci S, Pintucci F, Caiazza S, et al. The dacron felt colonizable keratoprosthesis: after 15 years. *Eur J Ophthalmol* 1996; 6: 125–130.
27. Chirila TV. An overview of the development of artificial corneas with porous skirts and the use of PHEMA for such an application. *Biomaterials* 2001; 22: 3311–3317.
28. Hicks CR, Chirila TV, Werner L, et al. Deposits in artificial corneas: risk factors and prevention. *Clin Exp Ophthalmol* 2004; 32: 185–191.
29. Strampelli B. Keratoprosthesis with osteoodontal tissue. *Am J Ophthalmol* 1963; 89: 1029–1039.
30. Casey TA. Osteo-odonto-keratoprosthesis. *Proc R Soc Med* 1966; 59: 530–531.
31. Falcinelli G, Falsini B, Taloni M, et al. Modified osteo-odonto-keratoprosthesis for treatment of corneal blindness: long-term anatomical and functional outcomes in 181 cases. *Arch Ophthalmol* 2005; 123: 1319–1329.
32. Temprano J. Keratoprosthesis with tibial autograft. *Refract Corn Surg* 1993; 9: 192.
33. Charoenrook V, Michael R, de la Paz MF, et al. Osteokeratoprosthesis using tibial bone: surgical technique and outcomes. *Ocul Surf* 2016; 14: 495–506.
34. Hille K, Hille A and Ruprecht KW. Medium term results in keratoprostheses with biocompatible and biological haptic. *Graefes Arch Clin Exp Ophthalmol* 2006; 244: 696–704.
35. Pintucci S, Perilli R, Formisano G, et al. Influence of dacron tissue thickness on the performance of the pintucci biointegrable keratoprosthesis: an in vitro and in vivo study. *Cornea* 2001; 20: 647–650.
36. Maskati QB and Maskati BT. Asian experience with the pintucci keratoprosthesis. *Indian J Ophthalmol* 2006; 54: 89–94.
37. Avadhanam VS and Liu CS. A brief review of Boston type-1 and osteo-odonto keratoprostheses. *Br J Ophthalmol* 2015; 99: 878–887.
38. Avadhanam VS, Smith HE and Liu C. Keratoprostheses for corneal blindness: a review of contemporary devices. *Clin Ophthalmol* 2015; 9: 697–720.
39. Liu C, Paul B, Tandon R, et al. The osteo-odonto-keratoprosthesis (OOKP). *Semin Ophthalmol* 2005; 20: 113–128.
40. Hille K, Grabner G, Liu C, et al. Standards for modified osteoodontokeratoprosthesis (OOKP) surgery according to strampelli and falcinelli: the Rome-Vienna protocol. *Cornea* 2005; 24: 895–908.
41. Strampelli B. Keratoprosthesis with osteoodontal tissue. *Am J Ophthalmol* 1963; 89: 1029–1039.
42. Barber JC. Keratoprosthesis: past and present. *Int Ophthalmol Clin* 1988; 28: 103–109.
43. Legeais JM, Renard G, Parel JM, et al. Expanded fluorocarbon for keratoprosthesis cellular ingrowth and transparency. *Exp Eye Res* 1994; 58: 41–51.
44. Chirila TV, Vijayasekaran S, Horne R, et al. Interpenetrating polymer network (ipn) as a permanent joint between the elements of a New-Type of artificial cornea. *J Biomed Mater Res* 1994; 28: 745–753.
45. Hicks CR, Crawford GJ, Dart JKG, et al. AlphaCor – clinical outcomes. *Cornea* 2006; 25: 1034–1042.
46. Todani A, Ciolino JB, Ament JD, et al. Titanium back plate for a PMMA keratoprosthesis: clinical outcomes. *Graefes Arch Clin Exp Ophthalmol* 2011; 249: 1515–1518.
47. Doane MG, Dohlman CH and Bearse G. Fabrication of a keratoprosthesis. *Cornea* 1996; 15: 179–184.
48. Carlsson DJ, Li F, Shimmura S, et al. Bioengineered corneas: how close are we? *Curr Opin Ophthalmol* 2003; 14: 192–197.
49. Cruise GM, Scharp DS and Hubbell JA. Characterization of permeability and network structure of interfacially photopolymerized poly(ethylene glycol) diacrylate hydrogels. *Biomaterials* 1998; 19: 1287–1294.
50. Nguyen KT and West JL. Photopolymerizable hydrogels for tissue engineering applications. *Biomaterials* 2002; 23: 4307–4314.
51. Wallace C, Jacob JT, Stoltz A, et al. Corneal epithelial adhesion strength to tethered-protein/peptide modified hydrogel surfaces. *J Biomed Mater Res A* 2005; 72: 19–24.
52. Jiraskova N, Rozsival P, Burova M, et al. AlphaCor artificial cornea: clinical outcome. *Eye (Lond)* 2011; 25: 1138–1146.
53. Pino M, Stingelin N and Tanner KE. Nucleation and growth of apatite on NaOH-treated PEEK, HDPE and UHMWPE for artificial cornea materials. *Acta Biomater* 2008; 4: 1827–1836.
54. Viitala R, Franklin V, Green D, et al. Towards a synthetic osteo-odonto-keratoprosthesis. *Acta Biomater* 2009; 5: 438–452.
55. Tan XW, Perera AP, Tan A, et al. Comparison of candidate materials for a synthetic osteo-odonto keratoprosthesis device. *Invest Ophthalmol Vis Sci* 2011; 52: 21–29.
56. Tan XW, Thompson B, Konstantopoulos A, et al. Application of graphene as candidate biomaterial for synthetic keratoprosthesis skirt. *Invest Ophthalmol Vis Sci* 2015; 56: 6605–6611.
57. Huhtinen R, Sandeman S, Rose S, et al. Examining porous bio-active glass as a potential osteo-odonto-keratoprosthetic skirt material. *J Mater Sci Mater Med* 2013; 24: 1217–1227.
58. Duncker GIW, Storsberg J and Müller-Lierheim WGK. The fully synthetic, bio-coated MIRO® CORNEA UR keratoprosthesis: development, preclinical testing, and

first clinical results. *Spektrum Der Augenheilkunde* 2014; 28: 250–260.
59. Ciolino JB and Dohlman CH. Biologic keratoprosthesis materials. *Int Ophthalmol Clin* 2009; 49: 1–9.
60. Flowerlet M, Arya S, Mini A, et al. Hydrogel – a drug delivery device. *Int J Univ Pharm Bio Sci* 2014; 3: 2–4.
61. Gong JP, Katsuyama Y, Kurokawa T, et al. Double-Network hydrogels with extremely high mechanical strength. *Adv Mater* 2003; 15: 1155–1158.
62. Ingavle G, Avadhanam V, Zheng Y, et al. Biomineralised interpenetrating network hydrogels for bone tissue engineering. *Bioinspired Biomimetic Nanobiomater* 2016; 5: 12–23.
63. DeKosky BJ, Dormer NH, Ingavle GC, et al. Hierarchically designed agarose and poly(ethylene glycol) interpenetrating network hydrogels for cartilage tissue engineering. *Tissue Eng Part C Methods* 2010; 16: 1533–1542.
64. Ingavle GC, Dormer NH, Gehrke SH, et al. Using chondroitin sulfate to improve the viability and biosynthesis of chondrocytes encapsulated in interpenetrating network (IPN) hydrogels of agarose and poly(ethylene glycol) diacrylate. *J Mater Sci Mater Med* 2012; 23: 157–170.
65. Ingavle GC, Frei AW, Gehrke SH, et al. Incorporation of aggrecan in interpenetrating network hydrogels to improve cellular performance for cartilage tissue engineering. *Tissue Eng Part A* 2013; 19: 1349–1359.
66. Ingavle GC, Gehrke SH and Detamore MS. The bioactivity of agarose-PEGDA interpenetrating network hydrogels with covalently immobilized RGD peptides and physically entrapped aggrecan. *Biomaterials* 2014; 35: 3558–3570.
67. Dhivya S, Saravanan S, Sastry TP, et al. Nanohydroxyapatite-reinforced chitosan composite hydrogel for bone tissue repair in vitro and in vivo. *J Nanobiotechnol* 2015; 13: 3558–3570.
68. Isikli C, Hasirci V and Hasirci N. Development of porous chitosan-gelatin/hydroxyapatite composite scaffolds for hard tissue-engineering applications. *J Tissue Eng Regen Med* 2012; 6: 135–143.
69. Na K, Kim SW, Sun BK, et al. Osteogenic differentiation of rabbit mesenchymal stem cells in thermo-reversible hydrogel constructs containing hydroxyapatite and bone morphogenic protein-2 (BMP-2). *Biomaterials* 2007; 28: 2631–2637.
70. Venugopal J, Prabhakaran MP, Zhang Y, et al. Biomimetic hydroxyapatite-containing composite nanofibrous substrates for bone tissue engineering. *Philos Trans A Math Phys Eng Sci* 2010; 368: 2065–2081.
71. Chou L, Marek B and Wagner WR. Effects of hydroxylapatite coating crystallinity on biosolubility, cell attachment efficiency and proliferation in vitro. *Biomaterials* 1999; 20: 977–985.
72. Kilpadi KL, Chang PL and Bellis SL. Hydroxylapatite binds more serum proteins, purified integrins, and osteoblast precursor cells than titanium or steel. *J Biomed Mater Res* 2001; 57: 258–267.
73. Murphy WL, Kohn DH and Mooney DJ. Growth of continuous bonelike mineral within porous poly (lactide-co-glycolide) scaffolds in vitro. *J Biomed Mater Res* 2000; 50: 50–58.
74. Sandeman SR, Lloyd AW, Tighe BJ, et al. A model for the preliminary biological screening of potential keratoprosthetic biomaterials. *Biomaterials* 2003; 24: 4729–4739.
75. Murphy WL and Messersmith PB. Compartmental control of mineral formation: adaptation of a biomineralization strategy for biomedical use. *Polyhedron* 2000; 19: 357–363.
76. Elliott JC. *Structure and chemistry of the apatites and other calcium orthophosphates*. New York: Elsevier, 1994.
77. Avadhanam VS, Zarei-Ghanavati M, Bardan AS, et al. When there is no tooth – looking beyond the falcinelli MOOKP. *Ocul Surf* 2019; 17: 4–8.
78. Lutolf MP and Hubbell JA. Synthetic biomaterials as instructive extracellular microenvironments for morphogenesis in tissue engineering. *Nat Biotechnol* 2005; 23: 47–55.
79. Kopecek J and Yang JY. Review – hydrogels as smart biomaterials. *Polym Int* 2007; 56: 1078–1098.
80. Rennerfeldt DA, Renth AN, Talata Z, et al. Tuning mechanical performance of poly(ethylene glycol) and agarose interpenetrating network hydrogels for cartilage tissue engineering. *Biomaterials* 2013; 34: 8241–8257.
81. Kokubo T, Ito S, Huang ZT, et al. Ca,P-rich layer formed on high-strength bioactive glass-ceramic A-W. *J Biomed Mater Res* 1990; 24: 331–343.
82. Trommer RM, Santos LA and Bergmann CP. Alternative technique for hydroxyapatite coatings. *Surf Coatings Technol* 2007; 201: 9587–9593.
83. Amling M, Schilling AF, Pogoda P, et al. The physiologic process required for biologization of bone substitutes. *Eur J Trauma* 2006; 32: 102–106.
84. Kim MK, Lee JL, Wee WR, et al. Seoul-type keratoprosthesis: preliminary results of the first 7 human cases. *Arch Ophthalmol* 2002; 120: 761–766.
85. Lee WB, Shtein RM, Kaufman SC, et al. Boston keratoprosthesis: outcomes and complications: a report by the American Academy of Ophthalmology. *Ophthalmology* 2015; 122: 1504–1511.
86. Riau AK, Venkatraman SS, Dohlman CH, et al. Modifications of the PMMA optic of a keratoprosthesis to improve biointegration. *Cornea* 2017; 36: S15–S25.
87. Legeais JM and Renard G. A second generation of artificial cornea (biokpro II). *Biomaterials* 1998; 19: 1517–1522.
88. Zarei-Ghanavati S, Betancurt C, Mas AM, et al. Ultra high resolution optical coherence tomography in Boston type I keratoprosthesis. *J Ophthalmic Vis Res* 2015; 10: 26–32.
89. Ghaffariyeh A, Honarpisheh N, Karkhaneh A, et al. Fyodorov-Zuev keratoprosthesis implantation: long-term results in patients with multiple failed corneal grafts. *Graefes Arch Clin Exp Ophthalmol* 2011; 249: 93–101.